Virologica Sinica 38 (2023) 559–567

Contents lists available at ScienceDirect

Virologica Sinica

journal homepage: www.keaipublishing.com/en/journals/virologica-sinica
www.virosin.org

Research Article

PA-E18G substitution in influenza A virus confers resistance to ZX-7101, a cap-dependent endonuclease inhibitor

Dan Luo [a,1], Qing Ye [a,1], Rui-Ting Li [a,1], Hang-Yu Zhou [b,1], Jing-Jing Guo [a], Suo-Qun Zhao [a], Sen Zhang [a], Tao Jiang [a], Yong-Qiang Deng [a,*], Cheng-Feng Qin [a,*]

[a] State Key Laboratory of Pathogen and Biosecurity, Beijing Institute of Microbiology and Epidemiology, Academy of Military Medical Sciences, Beijing 100071, China
[b] State Key Laboratory of Medical Molecular Biology, Suzhou Institute of Systems Medicine, Chinese Academy of Medical Sciences & Peking Union Medical College, Suzhou 215123, China

ARTICLE INFO

Keywords:
Influenza virus
Cap-dependent endonuclease (CEN)
Baloxavir marboxil (BXM)
Drug resistance

ABSTRACT

Cap-dependent endonuclease (CEN) in the polymerase acidic protein (PA) of influenza A virus (IAV) represents a promising drug target due to its critical role in viral gene transcription. The CEN inhibitor, baloxavir marboxil (BXM), was approved in Japan and the US in 2018 and several other countries subsequently. Along with the clinical use of BXM, the emergence and spread of IAV variants with reduced susceptibility to BXM have aroused serious concern. Herein, we comprehensively characterized the *in vitro* and *in vivo* antiviral activities of ZX-7101A, an analogue of BXM. The active form of prodrug ZX-7101 showed broad-spectrum antiviral potency against various IAV subtypes, including pH1N1, H3N2, H7N9 and H9N2, in MDCK cells, and the 50% effective concentration (EC_{50}) was calculated to nanomole level and comparable to that of baloxavir acid (BXA), the active form of BXM. Furthermore, *in vivo* assays showed that administration of ZX-7101A conferred significant protection against lethal pH1N1 challenge in mice, with reduced viral RNA loads and alleviated pulmonary damage. Importantly, serial passaging of H1N1 virus in MDCK cells under selection pressure of ZX-7101 led to a resistant variant at the 15th passage. Reverse genetic and sequencing analysis demonstrated that a single E18G substitution in the PA subunit contributed to the reduced susceptibility to both ZX-7101 and BXA. Taken together, our results not only characterized a new CEN inhibitor of IAV but also identified a novel amino acid substitution responsible for CEN inhibitor resistance, which provides critical clues for future drug development and drug resistance surveillance.

1. Introduction

Influenza A viruses (IAVs) are highly contagious respiratory pathogens that can cause severe illness and death in high-risk groups. Although current flu vaccine is supposed to be effective to most IAV types, the increase in the number of new subtypes may reduce the effectiveness of influenza vaccines (Bhat et al., 2022; Wu et al., 2021). In addition, the increased prevalence of mammalian-adapted and neuraminidase inhibitor (NAI)-resistant viruses may limit the effectiveness of currently available drugs (Hossain et al., 2021; Quan et al., 2018). Therefore, there is an urgent need to develop effective antiviral agents with novel mechanisms of action.

Since the synthesis of influenza virus proteins depends on the host cell translation system (Area et al., 2004; Engelhardt and Fodor, 2006), influenza virus mRNA requires both a 5′-cap-like structure and a 3′-poly (A) tail that can be recognized by the host cell translation apparatus, so the transcription of influenza virus mRNA relies on a unique and complex "cap-snatching" mechanism. In this process, short-cap oligomers (approximately 10–15 nt) from the host pre-mRNA are "snatched" by polymerase-based protein 2 (PB2), cleaved by cap-dependent endonuclease (CEN) in the polymerase acidic protein (PA) (Yuan et al., 2009), and then used by viral polymerase-based protein 1 (PB1) to initiate viral mRNA synthesis. The viral mRNA is further spliced as a host pre-mRNA and exported into the cytoplasm by the host cellular machinery (Reich et al., 2014). The cleavage of CEN is an essential step in the mRNA synthesis process of influenza virus, and there is no enzyme with a similar mechanism of action in host cells; hence, CEN is considered to be a promising anti-influenza target.

* Corresponding authors.
E-mail addresses: dengyq1977@126.com (Y.-Q. Deng), qincf@bmi.ac.cn (C.-F. Qin).
[1] Dan Luo, Qing Ye, Rui-Ting Li, and Hang-Yu Zhou contributed equally to this work.

https://doi.org/10.1016/j.virs.2023.06.002
Received 26 January 2023; Accepted 5 June 2023
Available online 7 June 2023

A series of CEN inhibitors have been comprehensively characterized. In particular, baloxavir marboxil (BXM), a prodrug of baloxavir acid (BXA), is a founding member of the CEN inhibitor class that has demonstrated high potency against various IAVs *in vitro* with the 90% effective concentrations (EC_{90}) less than 10 nmol/L (Noshi et al., 2018). BXM also exhibited strong antiviral effects in mice and ferret models (Koszalka et al., 2022; Park et al., 2021). BXM was licenced in 2018 in the USA and Japan for the treatment of influenza (Baker et al., 2020; Ison et al., 2020). RO-7, an analogue of BXM, exhibited broad-spectrum activity against IAVs *in vitro* assays with the 50% effective concentrations (EC_{50}) at nanomolar concentrations (Jones et al., 2016). RO-7 treatment also significantly decreased virus titers in the lung and lessened the extent and severity of lung damage in the mouse model (Jones et al., 2017). AL-794 (also known as ALS-033794/JNJ-64155806), is an orally active prodrug of ALS-033719. ALS-033719 had an inhibitory effect on multiple IAVs, with EC_{90} ranging from 2.3 to 267 nmol/L (Yogaratnam et al., 2019). However, the exposure levels of AL-794 varied significantly based on prior food consumption and gender, and because a single dose which was both well-tolerated and effective against influenza virus infection could not be established, the development of the drug has been discontinued (Mifsud et al., 2019).

Along the use of CEN-inhibitors, the emergence of CEN inhibitor resistant variants as well as the underlying mechanism have been well documented. Noshi et al. isolated a variant with reduced BXA susceptibility by serial passages of the H1N1 viruses in the presence of BXA, and determined that the PA-I38T substitution was responsible for reduced BXA susceptibility by reverse genetics (Noshi et al., 2018). Moreover, a PA-E23K mutants was detected from a child without BXM treatment (Takashita et al., 2020a). Introduction of the PA-E23K into H1N1 virus by reverse genetics confirmed that the E23K substitution resulted in decreased susceptibility to BXA (Jones et al., 2022). Serial passage of H1N1 viruses in MDCK cells under selective pressure of RO-7 also identified a PA-I38T substitution, and recombinant H1N1 with the I38T substitution showed RO-7 resistance (Jones et al., 2018).

In present study, we aimed to systematically evaluate the *in vitro* and *in vivo* antiviral efficacy of a new BXM analogue ZX-7101A (profrug form) against various IAVs, and identify critical amino acid substitution responsible for CEN inhibitor resistance in order to provide critical clues for future drug development and drug resistance surveillance.

2. Materials and methods

2.1. Compounds

ZX-7101A, ZX-7101, BXA and BXM were synthesized by ZENSHINE Pharmaceutical Co., Ltd., Nanjing, China. Oseltamivir acid purchased from TargetMol Chemicals Inc. (Shanghai, China).

2.2. Cells, mice and viruses

The Madin-Darby canine kidney cell line MDCK (ATCC, Cat no. CCL-34), human embryonic kidney cell line HEK293T (ATCC, Cat no. CRL-3216) and human alveolar epithelial cell line A549 (ATCC, Cat no. CCL-185) were cultured in Dulbecco's modified Eagle's medium (Gibco/Invitrogen, Cat no. 2307629) with 10% fetal bovine serum (Gibco/Invitrogen, Cat no. 2517395), 1% penicillin streptomycin (Gibco/Invitrogen, Cat no. 2240831) and 1% HEPES (1 mol/L) (Gibco/Invitrogen, Cat no. 2185833) at 37 °C in a humidified atmosphere of 5% CO_2. Female BALB/c mice aged 5–6 weeks were purchased from Vital River Laboratory.

The influenza A viruses A/California/07/2009 (pH1N1), A/WSN/33 (H1N1), A/Wujiaqu/XJ58/2017 (H3N2), A/Anhui/1/2013 (H7N9), and A/Chicken/Nanjing/1/2013 (H9N2) (Nian et al., 2016) were grown and titrated according to the standard tissue culture infectious dose ($TCID_{50}$) in MDCK cells.

2.3. Enzyme inhibition assay

The enzyme inhibition assay has been described previously (Noshi et al., 2018). Influenza virus CEN PA_N (Pharmaron Inc, China) and influenza PA ssDNA substrates (5′FAM-AATCGCAGGCAGCACTC-3′TAMRA, Shanghai GeneRay Biotech Co., Ltd.) were used to determine the inhibitory activity of BXA, BXM, ZX-7101 and ZX-7101A on CEN of influenza virus *in vitro* (Credille et al., 2019). The influenza virus CEN PA_N (100 nmol/L) was mixed with compounds at different concentrations in a plate, centrifuged at 200×*g* speed for 60 s at 25 °C, and incubated at 25 °C for 20 min. Then, influenza PA ssDNA substrate (600 nmol/L) was added to all the wells in the dark and incubated at 37 °C for 4 h. The plate was removed and allowed to stand at 25 °C for 10 min and centrifuged at 200×*g* speed for 60 s. A Victor Nivo system was used to read the fluorescence values (Ex/Em = 485 nm/535 nm) and collect data. Data were processed with GraphPad Prism 7.00 software to calculate the 50% maximal inhibitory concentration (IC_{50}) values of the compounds. Inhibition rate = [1-(Fluorescence values - $Mean_{Min}$)/($Mean_{Max}$ - $Mean_{Min}$)] × 100%, Min: 1000 nmol/L Baloxavir acid, Max: 0.1% dimethyl sulfoxide (DMSO).

2.4. CellTiter-Glo® cell viability assay

The CellTiter-Glo® Cell Viability Assay (Promega, Cat no. G7573) was employed to evaluate the cytotoxicity and antiviral activity of drugs according to the manufacturer's protocols.

For cytotoxicity assays, MDCK cells were treated with different doses of either compound or DMSO in quadruplicate. Luminescence was recorded after three days of incubation at 37 °C, and the cytotoxic concentration (CC_{50}) was calculated using a sigmoidal nonlinear regression function to fit the dose-response curve using GraphPad Prism 7.0 software.

For antiviral activity, MDCK cells were seeded in a 96-well plate at a density of 2×10^4 cells/well and infected with 50 μL of a 100 $TCID_{50}$ virus suspension and another 50 μL of drug dilution. The cells were then incubated at 37 °C for 48 h. Cell viability was quantified as described above. All drug concentrations were measured with at least three replicates. Data were processed with GraphPad Prism 7.0 software to calculate the EC_{50} values of the compounds.

2.5. Immunofluorescence assay

MDCK cells infected with 100 $TCID_{50}$ of pH1N1 were co-cultured with ZX-7101 at 37 °C. After 12 h, the cells were collected and fixed with 4% paraformaldehyde and permeabilized with 0.5% Triton X-100. Then, the cells were incubated with the Influenza A virus NP antibody (GeneTex, Cat no. GTX125989) for 12 h at 4 °C, followed by incubation with the secondary antibody (ZSGB-BIO, Cat no. ZF-0511) for 1 h at 37 °C. The nuclei were stained with DAPI (Solarbio, Cat no. C0060) for 5 min at 25 °C. Images were captured by fluorescence microscopy.

2.6. Antiviral activity of ZX-7101A against influenza virus in mice

BALB/c female mice were anesthetized using diethyl ether and intranasally challenged with virus suspension (1000 PFU of pH1N1 in 30 μL of PBS). Diluted compounds were given orally once per day from day 1 to day 7. Animal weight and survival were monitored daily, and mice were euthanized until the end of the experiment or when body-weight lost more than 25%.

2.7. Histopathology assay

Haematoxylin and eosin (HE) staining was performed to evaluate the structural integrity and degree of inflammation of mouse tissue. For histopathology, mouse lungs were collected and fixed in 4% neutral-

buffered formaldehyde, embedded in paraffin, sectioned, and stained with haematoxylin and eosin. Images were captured with a microscope.

2.8. RNAscope in situ hybridization

RNAscope *in situ* hybridization was used to detect the expression of pH1N1. Briefly, the tissues were removed and fixed in 4% paraformaldehyde for 24 h. After fixation, the tissues were decalcified with 10% EDTA solution and embedded with paraffin wax. The slides were then treated using an Advanced Cell Diagnostics (ACD) RNAscope®2.5 HD Reagent Kit and RNAscope®Probe-V-InfluenzaA-H1N1-segment5-NP to detect pH1N1 infection. Positive (RNAscopeÒ 3-plex LS Multiplex Control Positive Probe-Mm polr2A, ppib, ubc; ACD) and negative (RNAscopeÒ 3-plex LS Multiplex Negative Control Probe dapB; ACD) controls were performed in parallel. After warming, dewaxing and rehydration, the slides were prepared using RNAscope target retrieval at 95 °C for 15 min. Probe hybridization and signal amplification were performed according to the manufacturer's instructions at 40 °C in a HybEZ hybridization oven, followed by counterstaining with haematoxylin.

2.9. RNA-seq analysis

A549 cells were infected with pH1N1 for 1 h. The cells were then treated with ZX-7101 (10 nM) for 48 h. Total RNA was extracted at 48 hpi by using TRIzol reagent (ThermoFisher, Cat no. 15596026) according to the manufacturer's instructions. RNA library construction and high-throughput sequencing were performed by Beijing Annoroad Gene Technology Company on the Illumina platform. Clean reads were aligned to the human genome (hg19) using HISAT2 (v2.1.0). The number of reads mapped to each gene for each sample was counted by HTSeq v0.6.0. Differential expression analysis was performed using the R package DESeq2 (v1.30.1) with PADJ < 0.05 and $|\log2 \text{ fold change}| > 1$. Heatmaps were constructed using the R package pheatmap (v1.0.12). Gene Ontology Biological Process (GO-BP) analysis was performed with Metascape. Volcano plots and barplots were constructed using the ggplot2 (v3.3.5) package in R. The RNA-seq data reported in the present paper have been deposited to the NCBI Gene Expression Omnibus (GEO) datasets under accession number GSE225905.

2.10. Isolation and characterization of ZX-7101-resistant variants

MDCK cells were initially infected with A/WSN/33 (H1N1) virus at an MOI of 0.1 and cultured for three days with ZX-7101 at a concentration of 0.1 nmol/L. Then, the culture supernatants were diluted tenfold and sequentially passaged through fresh MDCK cells in the presence of 0.1 nmol/L ZX-7101. Viruses from the final passage were propagated once in the absence of ZX-7101, and the susceptibility of the passaged viruses to ZX-7101 was evaluated with the CellTiter-Glo® Cell Viability Assay in MDCK cells. The viral RNAs were extracted, and Sanger sequencing was performed to determine the sequence of the PA gene.

2.11. Generation of recombinant viruses by reverse genetics

The eight pHW2000-based plasmids used for the generation of recombinant A/WSN/33 (H1N1) viruses have been described previously (Hoffmann et al., 2000) and were kindly provided by Dr Jingfeng Wang (Institute of Systems Medicine, Chinese Academy of Medical Sciences). The E18G, E23K and I38T mutations were inserted into the PA gene using the Q5 site-directed mutagenesis kit (NEB; E0554S) and the following primers: E18G-F: 5′-ggaaaggcaatgaaaGAGTATGGAGAGGACCTG-3′; E18G-R: 5′-cgcaagctcgacaatcATCGGATTGAAGCATTGTC-3′; E23K-F: 5′-aagtatggagAGGACCTGAAAATCGAAACAAAC-3′; E23K-R: 5′-tttcattgcct TTTCCGCAAGCTCGACAA-3′; I38T-F: 5′-cactcacttgGAAGTGTGCTTCA TGTATTC-3′; and I38T-R: 5′-catgttgctgcAAATTTGTTTGTTTCGATT TTC-3′. The wild-type recombinant A/WSN/33 virus was generated using an eight-plasmid system based on pHW2000 by transfection into human HEK293T cells. The plasmid encoding the PA subunit of A/WSN/33 was substituted with the mutated PA plasmid to obtain recombinant viruses containing PA-E18G, -E23K and -I38T mutations. Each virus was passaged in MDCK cells. The presence of the E18G, E23K and I38T mutations was confirmed by Sanger sequencing.

2.12. Plaque assay

Confluent monolayers of MDCK cells (10^5 cells/well in a 12-well plate) were infected with virus at 37 °C. After 1 h of virus adsorption, cells were overlaid with DMEM containing 1% low melting point agarose and TPCK-treated trypsin (2 μg/mL) and then incubated at 37 °C for 2–3 days. Cells were fixed for 15 min at 25 °C with 4% paraformaldehyde. The agarose overlay was removed and stained for 10 min with 1% crystal violet in methanol. The number of plaques in each well was counted.

2.13. Statistical analysis

Statistical analyses were carried out using Prism software (GraphPad). All data are presented as the means ± standard deviations. The statistical significance of differences among groups was analysed using Student's *t*-test, two-way ANOVA, one-way ANOVA and the log-rank test. *, **, *** and **** indicate $P < 0.05$, $P < 0.01$, $P < 0.001$ and $P < 0.0001$, respectively.

3. Results

3.1. ZX-7101 suppresses influenza A virus infection by inhibiting cap-dependent endonuclease

ZX-7101A was synthesized as the prodrug of a CEN inhibitor that is metabolized to its active form ZX-7101 *in vivo*. An enzyme inhibition assay was used to determine the inhibitory activity of ZX-7101 and ZX-7101A against CEN of IAV, with BXA and BXM as control compounds. The results showed that both BXA and ZX-7101 inhibited CEN activity with similar IC_{50} values of 22.26 nmol/L and 21.72 nmol/L, respectively. In contrast, the IC_{50}s of BXM and ZX-7101A were 2.88 μmol/L and 1.86 μmol/L, respectively (Fig. 1A).

The antiviral activity of ZX-7101 was first evaluated by an immunofluorescence assay, and the results showed that ZX-7101 significantly reduced pH1N1 NP protein production in a dose-dependent manner (Fig. 1B). Then, to assess the *in vitro* broad-spectrum antiviral activity of ZX-7101, MDCK cells were infected with various subtypes of IAV in the presence of compounds. As expected, BXA exhibited high potency against various subtypes of IAV (Table 1). Similarly, ZX-7101 also demonstrated equivalent effectiveness compared to BXA, and the EC_{50}s of ZX-7101 against pH1N1, H3N2, H7N9 and H9N2 were 4.13 nmol/L (SI = 2263.92), 1.03 nmol/L (SI = 9077.67), 4.39 nmol/L (SI = 2129.84), and 2.74 nmol/L (SI = 3412.41), respectively (Fig. 1C). These results demonstrated that ZX-7101 is a potent CEN inhibitor with similar antiviral activity to that of BXA.

3.2. ZX-7101A provides protection against A/California/07/2009 (pH1N1) virus infection in mice

Next, the protective efficacy of ZX-7101A was assayed in a well-established mouse model (Huang et al., 2020). BALB/c female mice were intranasally infected with a lethal dose of pH1N1 virus (1000 PFU). Then, 5 mg/kg ZX-7101A or BXM was given orally after infection once per day from day 1 to day 7, and body weight changes and mortality were monitored for 14 days (Fig. 2A). As shown in Fig. 2B, all mice from the

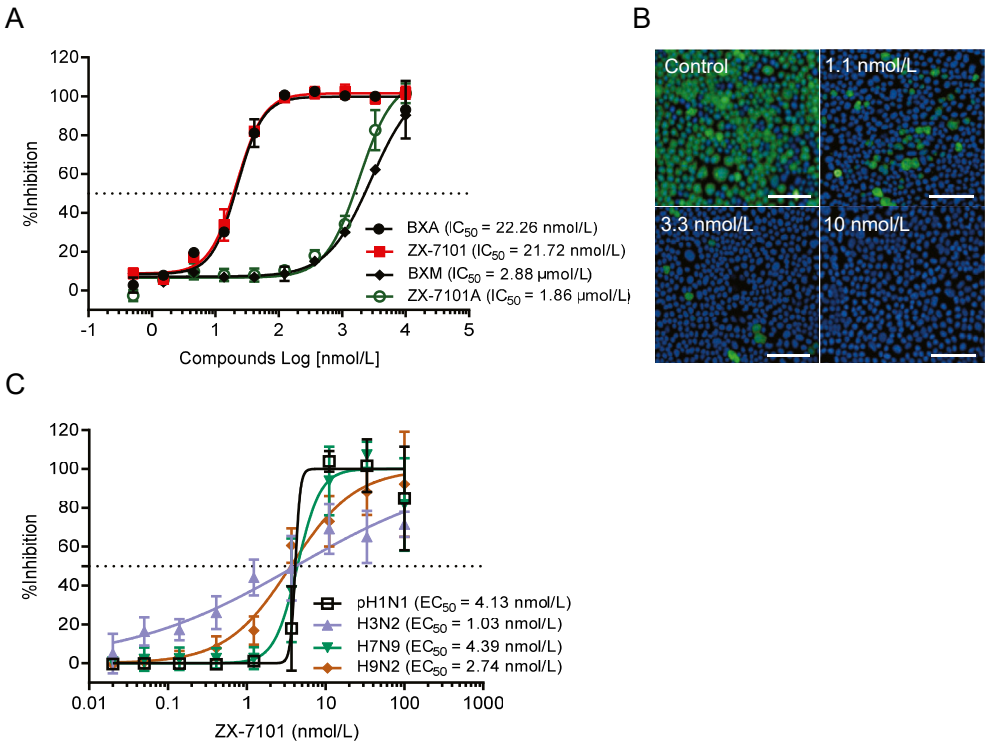

Fig. 1. Broad-spectrum antiviral potency of ZX-7101 against influenza virus *in vitro*. **A** Enzyme inhibition assay of cap-dependent endonuclease (CEN). The influenza virus CEN PA_N and influenza PA ssDNA substrate were used to determine the inhibitory activity of BXA, ZX-7101, BXM, and ZX-7101A against CEN of influenza virus *in vitro*. The fluorescence values (Ex/Em = 485 nm/535 nm) were recorded for inhibition activity analysis of the compounds. **B** Immunofluorescence assay of pH1N1-infected MDCK cells that received ZX-7101 treatment. MDCK cells infected with 100 $TCID_{50}$ of pH1N1 were co-cultured with ZX-7101 at 37 °C for 12 h. Cells were fixed and permeabilized for staining with an anti-viral NP antibody, followed by staining with Alexa 488-labelled secondary antibody. Green represents infected cells, and nuclei were stained with DAPI. Scale bar, 100 μm. **C** MDCK cells were infected with 100 $TCID_{50}$ of pH1N1, H3N2, H7N9, or H9N2. At the same time, different concentrations of ZX-7101 were added for coculture at 37 °C for 48 h. The inhibition potencies of the compounds were determined using a CellTiter-Glo® Luminescent Cell Viability Assay. The results are presented as the mean of four replicates ± SD.

vehicle group showed a decrease in body weight of more than 25% and died within 8 days. Treatment of ZX-7101A (5 mg/kg) provided protection for the mice from a significant body weight loss and death. The lung tissues of mice were collected at day 3 for RNAscope *in situ* hybridization detecting viral RNA and HE staining visualizing the inflammation. As expected, no viral RNA was detected in mock group; while large amounts of viral RNAs were detected in vehicle group (Fig. 2C). Treatment of ZX-7101A and BXM significantly decreased viral RNA loads in mouse lungs. HE staining (Fig. 2D) showed that pH1N1 infection led to typical influenza pneumonia involving inflammatory cell infiltrates, interstitial pneumonia and epithelial hyperplasia in the vehicle group. ZX-7101A and BXM treatment alleviated most pulmonary damage caused by pH1N1 infection compared with the vehicle group.

3.3. ZX-7101 treatment induced significant transcriptional changes

Next, to further profile the transcriptome-wide changes in response to ZX-7101 treatment, RNA-Seq was performed with pH1N1-infected A549 cells with or without ZX-7101 treatment (Fig. 3A). The results indicated that ZX-7101 treatment alone had little effect on cells and caused the differential expression of only two genes in A549 cells (Fig. 3B). However, pH1N1 infection resulted in the greatest degree of differential expression in A549 cells. A total of 3988 genes (2640 upregulated genes, 1348 downregulated genes) were significantly altered (Supplementary Fig. S1). In contrast, ZX-7101 treatment after pH1N1 virus infection caused only the upregulation of 104 genes and the downregulation of 278 genes (Fig. 3B). Gene Ontology (GO) enrichment analysis further

Table 1
Comparison of broad-spectrum anti-influenza virus potency of ZX-7101 with baloxavir acid and oseltamivir acid.

Compounds	Index	H1N1		H3N2	H7N9	H9N2
		(A/WSN/33)	pH1N1			
Baloxavir acid	EC_{50} (μmol/L)	0.00098	0.00306	0.00059	0.00692	0.00346
	CC_{50} (μmol/L)	8.11	8.11	8.11	8.11	8.11
	SI	8275.51	2650.33	13745.76	1171.97	2343.93
ZX-7101	EC_{50} (μmol/L)	0.001	0.00413	0.00103	0.00439	0.00274
	CC_{50} (μmol/L)	9.35	9.35	9.35	9.35	9.35
	SI	9350	2263.92	9077.67	2129.84	3412.41
Oseltamivir acid	EC_{50} (μmol/L)	1.158	17.57	1.557	20.39	11.69
	CC_{50} (μmol/L)	> 1000	> 1000	> 1000	> 1000	> 1000
	SI	> 863.56	> 56.91	> 642.26	> 49.04	> 85.54

EC_{50}s and CC_{50}s of the compounds were determined using a CellTiter-Glo® Luminescent Cell Viability Assay in MDCK cells. The CC_{50} of the compound was divided by EC_{50} to obtain the selection index (SI).

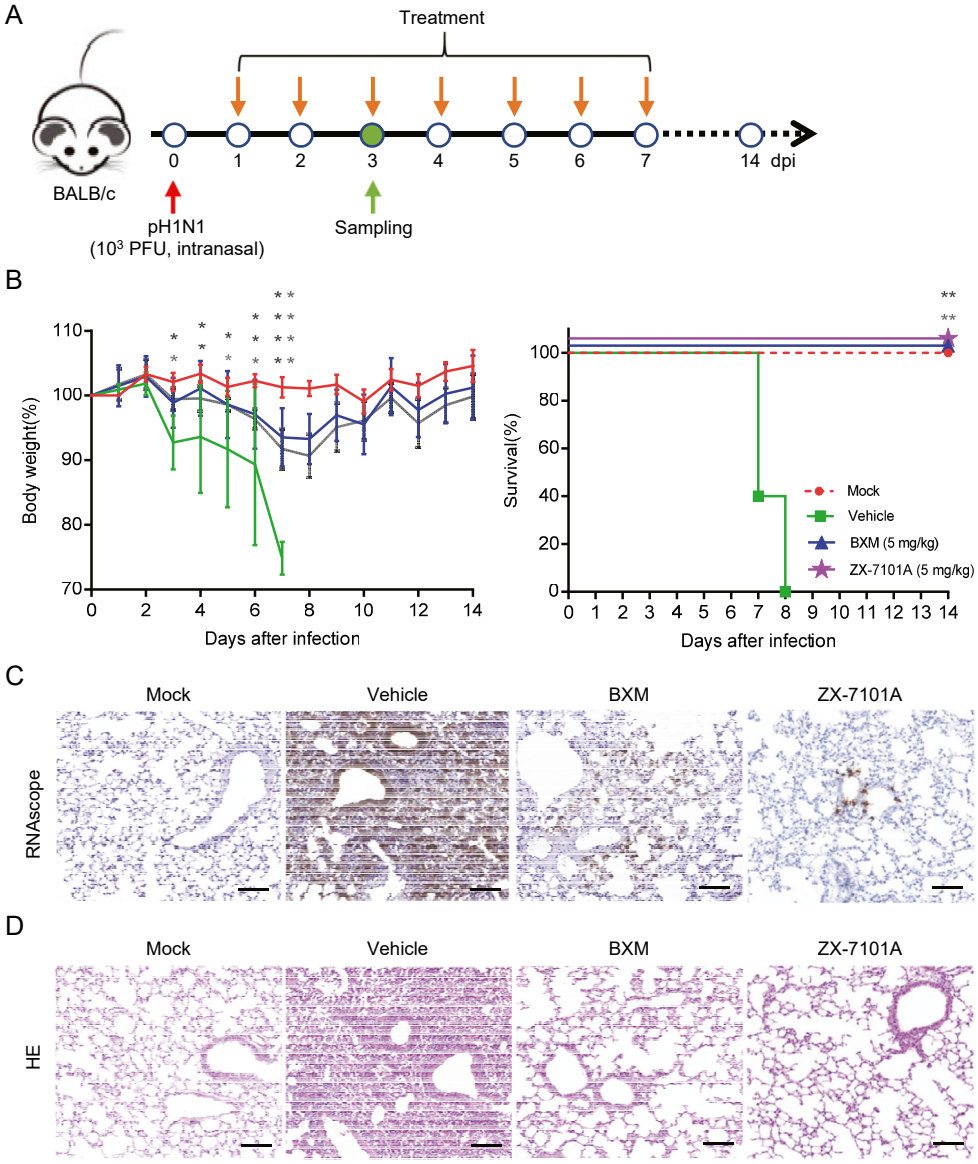

Fig. 2. The antiviral activity of ZX-7101A against influenza virus in mice. **A** Diagram of the experimental procedure. Briefly, BALB/c mice were randomly divided into an experimental group (ZX-7101A), a positive control drug group (BXM), a virus infection control group (Vehicle) and a blank control group (Mock). The mice were intranasally infected with the A/California/07/2009 (pH1N1) virus at 1000 PFU (5 LD_{50}), and the compounds were given orally once per day from day 1 to day 7. The dose of ZX-7101A, 5 mg/kg, was the same as that of BXM. The body weight and survival of mice were monitored until day 14, and mice were dissected and sampled on day 3 to detect the viral load and inflammatory response in mice. **B** Body weight loss and survival were monitored for 14 days or until the body weight decreased by more than 25% (n = 6 animals/group). Two-way ANOVA was used for body weight curves, and the log-rank test was used for survival curves. $^{*}P < 0.05$, $^{**}P < 0.01$, $^{****}P < 0.0001$. **C** Mouse lungs were fixed with 4% paraformaldehyde for RNAscope analysis to visualize pH1N1 NP mRNA (brown staining) at day 3. **D** Mouse lungs were stained with haematoxylin and eosin (HE) to show inflammatory response in the mouse lungs. Scale bar, 100 μm.

indicated that the major upregulated genes impacted by ZX-7101 were associated with innate immunity-related pathways, including the inflammatory response, leukocyte migration, and cytokine-mediated signalling. The downregulated genes were enriched in cell cycle-related terms, such as regulation of cell cycle process and DNA metabolic process (Fig. 3C, 3D). These results suggested that ZX-7101 could directly inhibit viral replication and therefore affected the expression of genes involved in inflammation and the cell cycle.

3.4. Isolation and characterization of ZX-7101-resistant variants

To further reveal the mechanism of action of ZX-7101, drug resistance selection was conducted as previously described (Noshi et al., 2018). Briefly, MDCK cells were infected with H1N1 virus and serially passaged for 15 rounds in the presence of 0.1 nmol/L ZX-7101 (Fig. 4A). Resistance analysis demonstrated that the virus from the 15th passage (H1N1-P15) exhibited 5-fold reduced susceptibility to ZX-7101 compared with wild-type H1N1 (Fig. 4B). H1N1-P15 also showed similar resistance to BXA (Fig. 4C). Specifically, $TCID_{50}$ assays confirmed that 1 nmol/L ZX-7101 and BXA, which showed obvious inhibitory effects against wild-type H1N1 viruses, had marginal antiviral effects against the H1N1-P15 virus (Fig. 4D). These results indicated that the H1N1-P15 variants were resistant to both ZX-7101 and BXA.

Sanger sequencing further revealed that the H1N1-P15 virus harboured a single nucleotide substitution of A to G at position 77, resulting in an amino acid substitution from Glu (E) to Gly (G) at position 18 of the

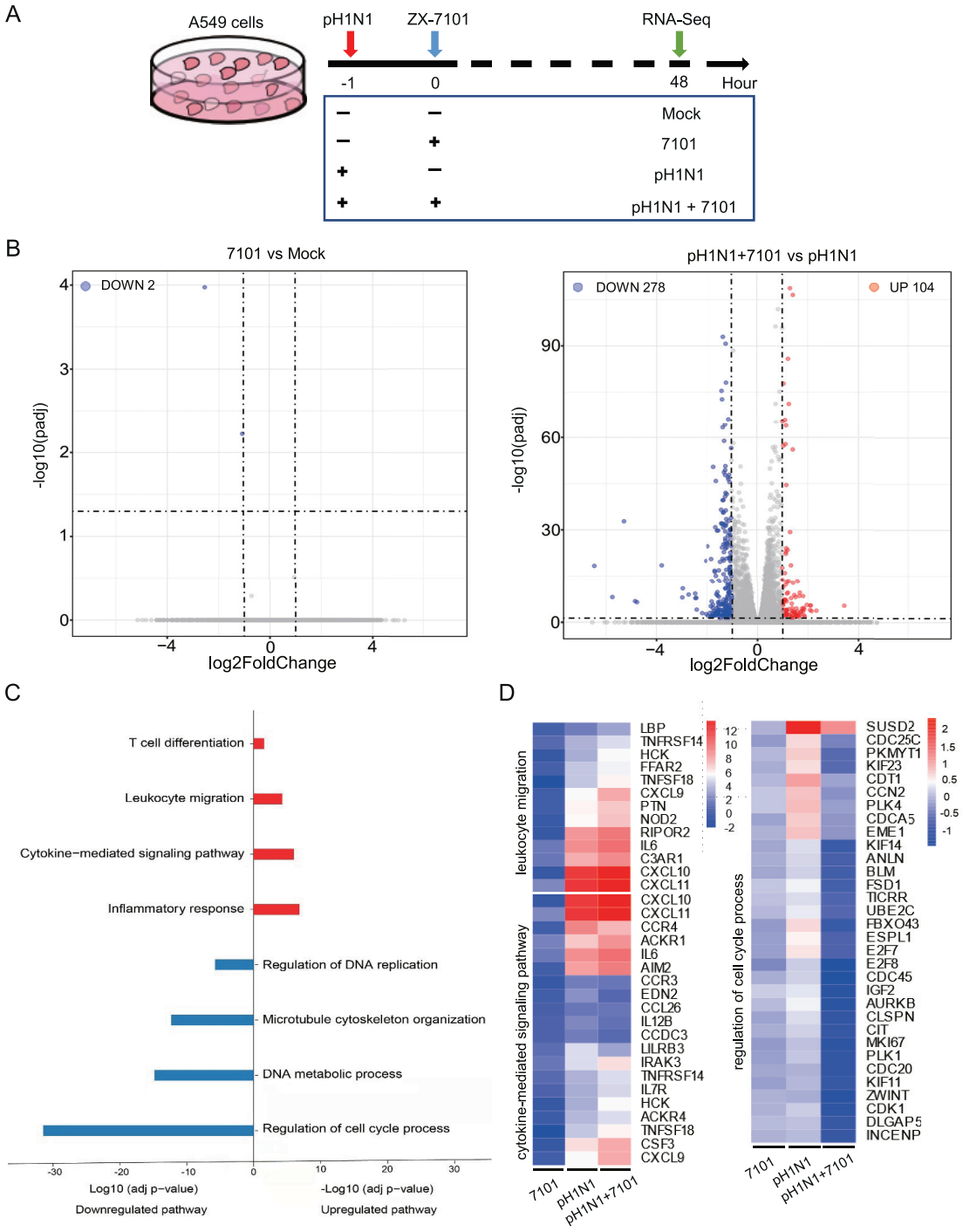

Fig. 3. Transcriptional analysis of ZX-7101 treatment. **A** Timeline of the transcriptomic study. A549 cells were infected with A/California/07/2009 (pH1N1) at an MOI of 0.1 before treatment with ZX-7101 or DMSO. The cell culture supernatant was collected for viral load determination, and A549 cells were collected at 48 hpi for transcriptional analysis. **B** Volcano plots indicating differentially regulated genes after ZX-7101 treatment with or without pH1N1 infection (pH1N1 + 7101 vs. pH1N1 and 7101 vs. mock). The numbers of downregulated and upregulated genes (PADJ <0.05 and |log2 fold change| > 1) are labelled in blue and red, respectively. **C** Gene Ontology Biological Process (GO-BP) analysis results for upregulated or downregulated genes comparing the pH1N1 + 7101- and pH1N1-treated groups. **D** Heatmaps of the genes enriched in the GO terms "leukocyte migration", "cytokine-mediated signalling pathway" and "regulation of cell cycle process". The colour depicts the log2 fold change compared with the mock group. Each cell represents the mean of three samples.

PA subunit. Notably, the aligning of amino acid sequence using NIH's protein blast tool [NCBI Blast:Protein Sequence (nih.gov)] showed that a total of 22 strains with G18 naturally in the PA subunit were found in various IAV subtypes, such as H1N1, H3N2, H4N6, H5N1, H5N2, H5N6, H6N2, H7N1 and H9N2 (Supplementary Table S1).

3.5. A single E18G substitution in PA contributes to reduced susceptibility to CEN inhibitors

To further clarify the role of the E18G substitution in the PA subunit, recombinant viruses containing the E18G substitution were generated by

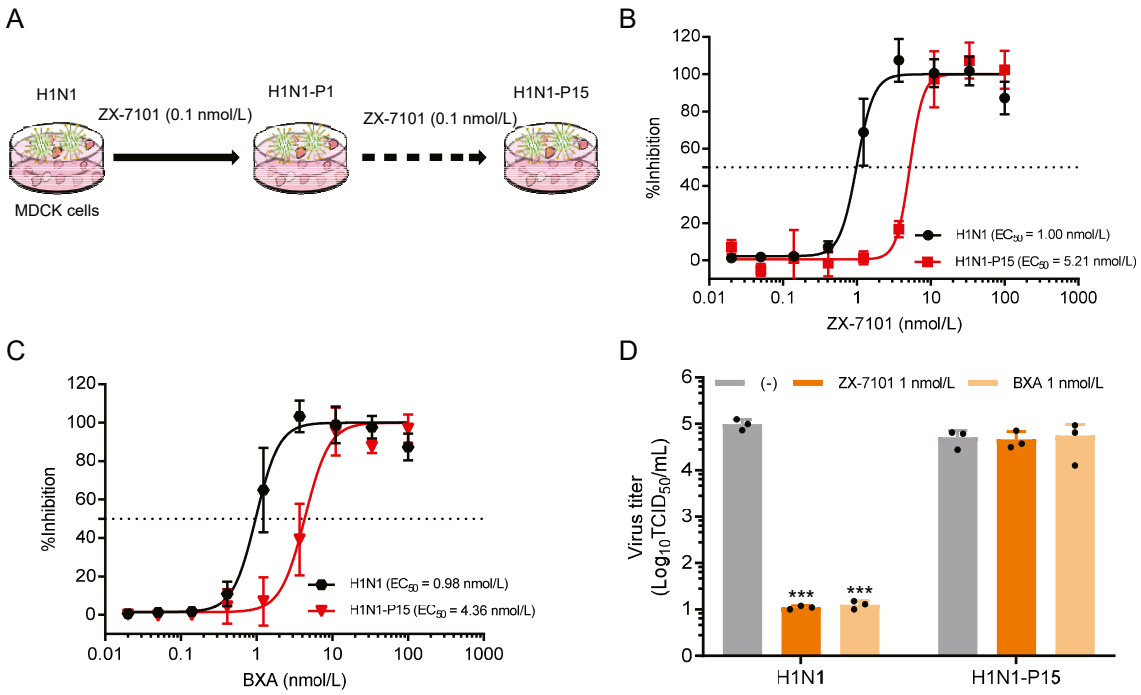

Fig. 4. Isolation and characterization of A/WSN/33 (H1N1) variants with reduced drug susceptibility. **A** Schematic representation of serial passage of the viruses for selecting ZX-7101-resistant virus. MDCK cells were initially infected with A/WSN/33 (H1N1) virus at an MOI of 0.1 and cultured with ZX-7101 at a concentration of 0.1 nmol/L for 3 days. The supernatants were diluted 10-fold and sequentially passaged through fresh MDCK cells in the presence of 0.1 nmol/L ZX-7101. **B, C** Susceptibility of variants to ZX-7101 and BXA by CellTiter-Glo® Luminescent Cell Viability Assay. MDCK cells were infected with 100 $TCID_{50}$ of H1N1 and H1N1-P15 variants. Then, different concentrations of ZX-7101 or BXA were added for coculture at 37 °C for 48 h. The inhibition potencies of the compounds were determined by CellTiter-Glo® Luminescent Cell Viability Assay. The results are presented as the mean of at least three replicates ± SD. **D** Susceptibility of variants to ZX-7101 and BXA by $TCID_{50}$ assay. MDCK cells infected with H1N1 or the H1N1-P15 variant at an MOI of 0.01 were treated with ZX-7101 (1 nmol/L) or BXA (1 nmol/L). After 48 h, supernatants were collected for $TCID_{50}$ assay in MDCK cells. The results are presented as the mean of three replicates ± SD. The black dots show the values from each experiment. ***$P < 0.001$. One-way ANOVA was used for virus titer.

standard reverse genetics technology using H1N1 (A/WSN/33) as the backbone (Fig. 5A). Two known BXM-resistance-associated substitutions, PA-E23K and -I38T (Ince et al., 2020), were constructed as controls. The standard multi-step growth curve showed that viral titers of PA-E18G viruses in the early phase of viral replication were comparable to wild type viruses, and were higher when compared to the PA-E23K and -I38T viruses in MDCK cells. In addition, the peak titers of the E18G viruses at 32 h post-infection were markedly higher compared to the wild type, E23K and I38T viruses (Fig. 5B). As expected, a plaque assay showed that the titers of the PA-WT virus were reduced by about 2 log PFU/mL in the presence of BXA and ZX-7101 at 5 nmol/L (Fig. 5C), while the titers of the PA-E18G and -E23K virus were reduced by about 1 and 0.6 log PFU/mL, respectively. The titers of the PA-I38T virus did not decrease (Fig. 5C). The EC_{50} values (Fig. 5D) of BXA and ZX-7101 for PA-WT virus were 0.70 nmol/L and 0.68 nmol/L, for PA-E23K virus were 12.23 nmol/L and 11.91 nmol/L, for PA-I38T virus were 27.92 nmol/L and 28.76 nmol/L, for PA-E18G virus were 6.87 nmol/L and 6.05 nmol/L. These results suggested that the PA-E18G substitution reduces susceptibility to CEN inhibitors.

4. Discussion

CEN in the PA subunit has become a promising anti-influenza target, and BXM represents the most successful example. In our study, we characterized a novel CEN inhibitor ZX-7101 *in vitro* and its prodrug form ZX-7101A *in vivo*. In enzymatic and cell-based assay, ZX-7101 showed a potent CEN inhibition comparable to BXA and exhibited broad-spectrum antiviral potency against various subtypes of IAV (EC_{50}s < 10 nmol/L). In influenza mouse model, ZX-7101A protected mice from pH1N1-related death and significantly reduced viral-induced pulmonary damage and inflammatory response, which is comparable to BXM (Dias et al., 2009; Noshi et al., 2018; Yuan et al., 2009).

Interestingly, transcriptional analysis indicated that ZX-7101 treatment upregulated a panel of genes involved in innate immunity-related pathways, including leukocyte migration and cytokine-mediated signalling pathways. These inflammatory responses were commonly impaired by viral infection (Music et al., 2016). ZX-7101 treatment also significantly downregulated the expression of genes related to the cell cycle. Previous results have indicated that host cell division favoured IAV protein accumulation and virus production (He et al., 2010; Jiang et al., 2013). Therefore, ZX-7101 exerts its antiviral effect by directly inhibiting viral replication as well as altering cellular responses to limit viral replication.

Characterization of viral mutants with reduced susceptibility may illustrate the molecular mechanism of action. In our study, we found that the PA-E18G substitution significantly decreased the susceptibility to ZX-7101 and BXA by 5- and 9-folds. Preclinical and clinical studies have identified multiple amino acid substitutions associated with reduced susceptibility to BXA (PA-E23 G/K/R, -A36V, -A37T, -I38 F/M/T/L, -E119D, -E199G) (Takashita et al., 2020b). While the PA-E18G substitution, to our knowledge, has not been reported before. Importantly, we found that IAVs with Gly18 exists naturally, such as A/Utah/13/2016(H1N1), A/California/MA_07/2009(H1N1), A/England/451/2009(H1N1), so attention should be paid to monitoring the E18G substitution.

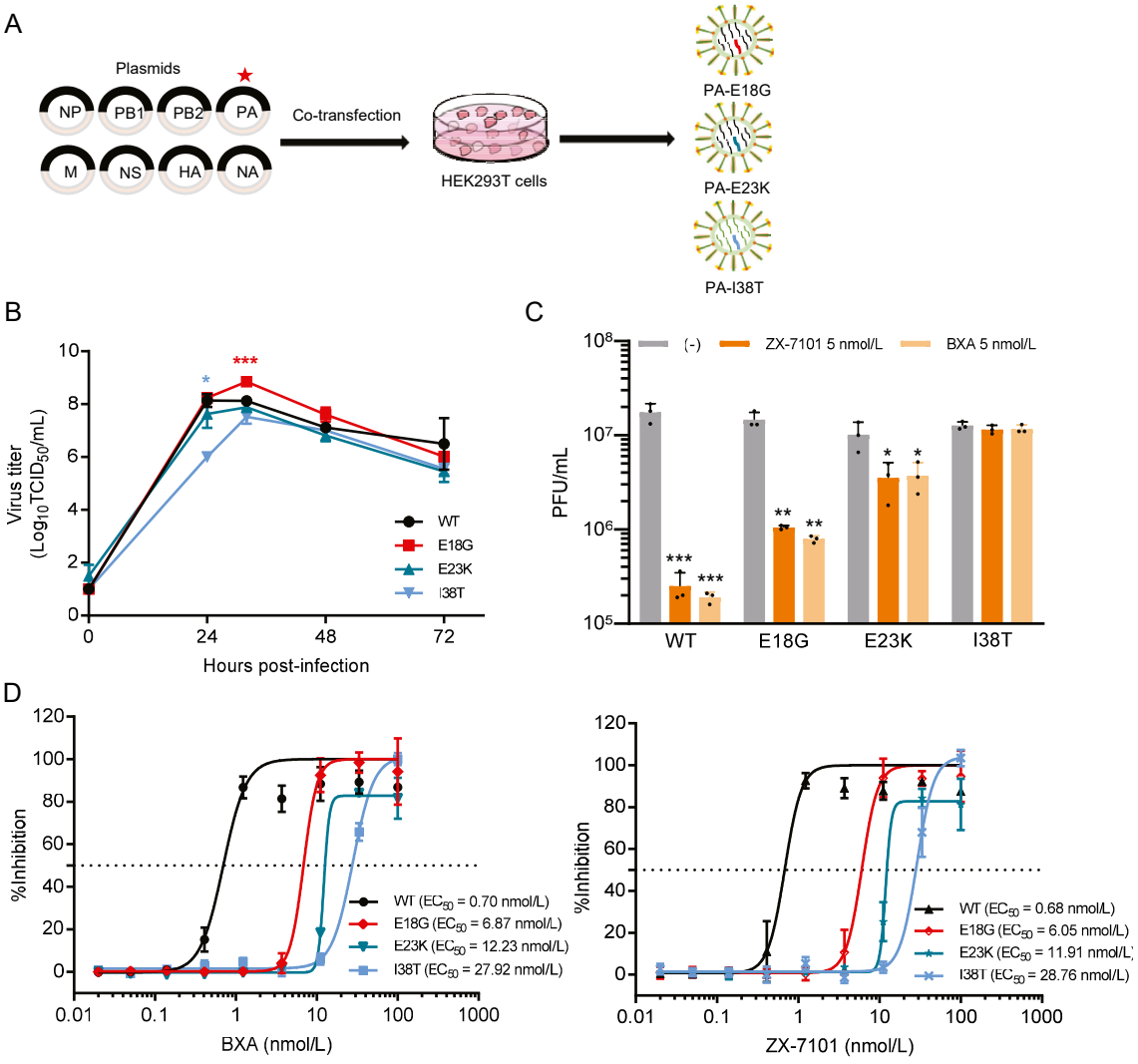

Fig. 5. Detection of ZX-7101 and BXA susceptibility of reverse genetics-derived viruses containing PA-E18G. **A** Construction of reverse genetics-derived viruses. Briefly, the *PA* gene of A/WSN/33 (H1N1) was recombined with the pHW2000 plasmid. The E18G, E23K and I38T mutations were inserted into the *PA* gene using the Q5 site-directed mutagenesis kit. The plasmid encoding the PA subunit of H1N1 was substituted with the mutated PA plasmid and was transfected into HEK293T cells to obtain the PA-E18G, -E23K and -I38T mutants using an eight-plasmid system. **B** The multi-step growth curve of PA-E18G, -E23K and -I38T virus. MDCK cells infected with wild type, PA-E18G, -E23K and -I38T virus at an MOI of 0.001, respectively. Supernatants were collected as indicated, and titers were determined by $TCID_{50}$ assay in MDCK cells. The results are presented as the mean of three replicates ± SD. $^{*}P < 0.05$, $^{***}P < 0.001$. Dunnett's multiple comparisons test was used for the multi-step growth curve. **C** Susceptibility of recombinant viruses to ZX-7101 and BXA by plaque assay. MDCK cells were infected with recombinant viruses at an MOI of 0.1 and incubated in the indicated concentration of ZX-7101 (5 nmol/L) or BXA (5 nmol/L). The supernatants were collected for plaque assays at day 2 post infection. The results are presented as the mean of three replicates ± SD. The black dots show the values from each experiment. $^{*}P < 0.05$, $^{**}P < 0.01$, $^{***}P < 0.001$. Student's *t*-test and Dunnett's multiple comparisons test were used for plaques number. **D** Susceptibility of recombinant viruses to ZX-7101 and BXA by CellTiter-Glo® Luminescent Cell Viability Assay. Briefly, MDCK cells were infected with 100 $TCID_{50}$ of the recombinant viruses above. Then, different concentrations of BXA or ZX-7101 were added for coculture at 37 °C for 48 h. The inhibition potencies of the compounds were determined by CellTiter-Glo® Luminescent Cell Viability Assay. The results are presented as the mean of three replicates ± SD.

5. Conclusions

In summary, we herein presented a new CEN inhibitor, ZX-7101, which was observed to successfully inhibit viral replication in cells. ZX-7101A also appears potent effective against pH1N1 challenge in mice. Furthermore, we discovered that a novel PA subunit E18G substitution, which could reduce susceptibility to ZX-7101 and BXA. Our data not only support the use of ZX-7101A as a new CEN inhibitor to clinically treat influenza in the future, but also help to elucidate the mechanism by which PA substitutions confer resistance to CEN inhibitors.

Data availability

All the data generated during the current study are included in the manuscript.

Ethics statement

This study was performed in strict accordance with the recommendations in the Guide for the Care and Use of Laboratory Animals of the Ministry of Science and Technology of the People's Republic of China. All animal experiments were approved by the Animal Experiment Committee of the Laboratory Animal Center, Beijing Institute of Microbiology and Epidemiology (approval number: IACUC-IME-2021-009).

Author contributions

Dan Luo: investigation, data curation, writing-original draft. Qing Ye: conceptualization, supervision. Rui-Ting Li: data curation. Hang-Yu Zhou: data curation. Jing-Jing Guo: data curation. Suo-Qun Zhao: methodology. Sen Zhang: data curation. Tao Jiang: data curation. Yong-

Qiang Deng: conceptualization, methodology, writing-review & editing, supervision. Cheng-Feng Qin: conceptualization, writing-review & editing, supervision. All authors read and approved the manuscript.

Conflict of interest

Prof. Cheng-Feng Qin is an editorial board member for *Virologica Sinica*, and was not involved in the editorial review or the decision to publish this article. All authors declare that there are no competing interests.

Acknowledgements

We thank ZENSHINE Pharmaceutical Co., Ltd., Nanjing, China, for providing the CEN inhibitors used in this study. The pHW2000 plasmid was kindly provided by Dr. Jingfeng Wang (Institute of Systems Medicine, Chinese Academy of Medical Sciences). This work was supported by the National Science and Technology Major Project (2018ZX097110003-005-002), the Key-Area Research and Development Program of Guangdong Province (2022B1111020002) and the National Natural Science Foundation of China (NSFC) (32170159, and 82174055). C.-F.Q. was supported by the National Science Fund for Distinguished Young Scholars (81925025), the Innovative Research Group (81621005) of the NSFC, and the Innovation Fund for Medical Sciences (2019-I2M-5-049) of the Chinese Academy of Medical Sciences.

Appendix A. Supplementary data

Supplementary data to this article can be found online at https://doi.org/10.1016/j.virs.2023.06.002.

References

Area, E., Martín-Benito, J., Gastaminza, P., Torreira, E., Valpuesta, J.M., Carrascosa, J.L., Ortín, J., 2004. 3D structure of the influenza virus polymerase complex: localization of subunit domains. Proc. Natl. Acad. Sci. U. S. A 101, 308–313.

Baker, J., Block, S.L., Matharu, B., Burleigh Macutkiewicz, L., Wildum, S., Dimonaco, S., Collinson, N., Clinch, B., Piedra, P.A., 2020. Baloxavir marboxil single-dose treatment in influenza-infected children: a randomized, double-blind, active controlled phase 3 safety and efficacy trial (miniSTONE-2). Pediatr. Infect. Dis. J. 39, 700–705.

Bhat, S., James, J., Sadeyen, J.R., Mahmood, S., Everest, H.J., Chang, P., Walsh, S.K., Byrne, A.M.P., Mollett, B., Lean, F., Sealy, J.E., Shelton, H., Slomka, M.J., Brookes, S.M., Iqbal, M., 2022. Coinfection of chickens with H9N2 and H7N9 avian influenza viruses leads to emergence of reassortant H9N9 virus with increased fitness for poultry and a zoonotic potential. J. Virol. 96, e0185621.

Credille, C.V., Morrison, C.N., Stokes, R.W., Dick, B.L., Feng, Y., Sun, J., Chen, Y., Cohen, S.M., 2019. SAR exploration of tight-binding inhibitors of influenza virus PA endonuclease. J. Med. Chem. 62, 9438–9449.

Dias, A., Bouvier, D., Crépin, T., McCarthy, A.A., Hart, D.J., Baudin, F., Cusack, S., Ruigrok, R.W., 2009. The cap-snatching endonuclease of influenza virus polymerase resides in the PA subunit. Nature 458, 914–918.

Engelhardt, O.G., Fodor, E., 2006. Functional association between viral and cellular transcription during influenza virus infection. Rev. Med. Virol. 16, 329–345.

He, Y., Xu, K., Keiner, B., Zhou, J., Czudai, V., Li, T., Chen, Z., Liu, J., Klenk, H.D., Shu, Y.L., Sun, B., 2010. Influenza A virus replication induces cell cycle arrest in G0/G1 phase. J. Virol. 84, 12832–12840.

Hoffmann, E., Neumann, G., Kawaoka, Y., Hobom, G., Webster, R.G., 2000. A DNA transfection system for generation of influenza A virus from eight plasmids. Proc. Natl. Acad. Sci. U. S. A 97, 6108–6113.

Hossain, M.G., Akter, S., Dhole, P., Saha, S., Kazi, T., Majbauddin, A., Islam, M.S., 2021. Analysis of the genetic diversity associated with the drug resistance and pathogenicity of influenza A virus isolated in Bangladesh from 2002 to 2019. Front. Microbiol. 12, 735305.

Huang, Y., Owino, S.O., Crevar, C.J., Carter, D.M., Ross, T.M., 2020. N-linked glycans and K147 residue on hemagglutinin synergize to elicit broadly reactive H1N1 influenza virus antibodies. J. Virol. 94, e01432-19.

Ince, W.L., Smith, F.B., O'Rear, J.J., Thomson, M., 2020. Treatment-emergent influenza virus polymerase acidic substitutions independent of those at I38 associated with reduced baloxavir susceptibility and virus rebound in trials of baloxavir marboxil. J. Infect. Dis. 222, 957–961.

Ison, M.G., Portsmouth, S., Yoshida, Y., Shishido, T., Mitchener, M., Tsuchiya, K., Uehara, T., Hayden, F.G., 2020. Early treatment with baloxavir marboxil in high-risk adolescent and adult outpatients with uncomplicated influenza (CAPSTONE-2): a randomised, placebo-controlled, phase 3 trial. Lancet Infect. Dis. 20, 1204–1214.

Jiang, W., Wang, Q., Chen, S., Gao, S., Song, L., Liu, P., Huang, W., 2013. Influenza A virus NS1 induces G0/G1 cell cycle arrest by inhibiting the expression and activity of RhoA protein. J. Virol. 87, 3039–3052.

Jones, J.C., Kumar, G., Barman, S., Najera, I., White, S.W., Webby, R.J., Govorkova, E.A., 2018. Identification of the I38T PA substitution as a resistance marker for next-generation influenza virus endonuclease inhibitors. mBio 9, e00430-18.

Jones, J.C., Marathe, B.M., Lerner, C., Kreis, L., Gasser, R., Pascua, P.N., Najera, I., Govorkova, E.A., 2016. A novel endonuclease inhibitor exhibits broad-spectrum anti-influenza virus activity in vitro. Antimicrob. Agents Chemother. 60, 5504–5514.

Jones, J.C., Marathe, B.M., Vogel, P., Gasser, R., Najera, I., Govorkova, E.A., 2017. The PA endonuclease inhibitor RO-7 protects mice from lethal challenge with influenza A or B viruses. Antimicrob. Agents Chemother. 61, e02460-16.

Jones, J.C., Zagribelnyy, B., Pascua, P.N.Q., Bezrukov, D.S., Barman, S., Okda, F., Webby, R.J., Ivanenkov, Y.A., Govorkova, E.A., 2022. Influenza A virus polymerase acidic protein E23G/K substitutions weaken key baloxavir drug-binding contacts with minimal impact on replication and transmission. PLoS Pathog. 18, e1010698.

Koszalka, P., George, A., Dhanasekaran, V., Hurt, A.C., Subbarao, K., 2022. Effect of baloxavir and oseltamivir in combination on infection with influenza viruses with PA/I38T or PA/E23K substitutions in the ferret model. mBio 13, e0105622.

Mifsud, E.J., Hayden, F.G., Hurt, A.C., 2019. Antivirals targeting the polymerase complex of influenza viruses. Antivir. Res. 169, 104545.

Music, N., Reber, A.J., Kim, J.H., York, I.A., 2016. Peripheral leukocyte migration in ferrets in response to infection with seasonal influenza virus. PLoS One 11, e0157903.

Nian, Q.G., Jiang, T., Zhang, Y., Deng, Y.Q., Li, J., Qin, E.D., Qin, C.F., 2016. High thermostability of the newly emerged influenza A (H7N9) virus. J. Infect. 72, 393–394.

Noshi, T., Kitano, M., Taniguchi, K., Yamamoto, A., Omoto, S., Baba, K., Hashimoto, T., Ishida, K., Kushima, Y., Hattori, K., Kawai, M., Yoshida, R., Kobayashi, M., Yoshinaga, T., Sato, A., Okamatsu, M., Sakoda, Y., Kida, H., Shishido, T., Naito, A., 2018. In vitro characterization of baloxavir acid, a first-in-class cap-dependent endonuclease inhibitor of the influenza virus polymerase PA subunit. Antivir. Res. 160, 109–117.

Park, J.H., Kim, B., Antigua, K.J.C., Jeong, J.H., Kim, C.I., Choi, W.S., Oh, S., Kim, C.H., Kim, E.G., Choi, Y.K., Baek, Y.H., Song, M.S., 2021. Baloxavir-oseltamivir combination therapy inhibits the emergence of resistant substitutions in influenza A virus PA gene in a mouse model. Antivir. Res. 193, 105126.

Quan, C., Shi, W., Yang, Y., Yang, Y., Liu, X., Xu, W., Li, H., Li, J., Wang, Q., Tong, Z., Wong, G., Zhang, C., Ma, S., Ma, Z., Fu, G., Zhang, Z., Huang, Y., Song, H., Yang, L., Liu, W.J., Liu, Y., Liu, W., Gao, G.F., Bi, Y., 2018. New threats from H7N9 influenza virus: spread and evolution of high- and low-pathogenicity variants with high genomic diversity in wave five. J. Virol. 92, e00301-e00318.

Reich, S., Guilligay, D., Pflug, A., Malet, H., Berger, I., Crépin, T., Hart, D., Lunardi, T., Nanao, M., Ruigrok, R.W., Cusack, S., 2014. Structural insight into cap-snatching and RNA synthesis by influenza polymerase. Nature 516, 361–366.

Takashita, E., Abe, T., Morita, H., Nagata, S., Fujisaki, S., Miura, H., Shirakura, M., Kishida, N., Nakamura, K., Kuwahara, T., Mitamura, K., Ichikawa, M., Yamazaki, M., Watanabe, S., Hasegawa, H., 2020a. Influenza A(H1N1)pdm09 virus exhibiting reduced susceptibility to baloxavir due to a PA E23K substitution detected from a child without baloxavir treatment. Antivir. Res. 180, 104828.

Takashita, E., Daniels, R.S., Fujisaki, S., Gregory, V., Gubareva, L.V., Huang, W., Hurt, A.C., Lackenby, A., Nguyen, H.T., Pereyaslov, D., Roe, M., Samaan, M., Subbarao, K., Tse, H., Wang, D., Yen, H.L., Zhang, W., Meijer, A., 2020b. Global update on the susceptibilities of human influenza viruses to neuraminidase inhibitors and the cap-dependent endonuclease inhibitor baloxavir, 2017-2018. Antivir. Res. 175, 104718.

Wu, Y., Hu, J., Jin, X., Li, X., Wang, J., Zhang, M., Chen, J., Xie, S., Qi, W., Liao, M., Jia, W., 2021. Accelerated Evolution of H7N9 Subtype Influenza Virus under Vaccination Pressure. Virol Sin 36, 1124–1132.

Yogaratnam, J., Rito, J., Kakuda, T.N., Fennema, H., Gupta, K., Jekle, C.A., Mitchell, T., Boyce, M., Sahgal, O., Balaratnam, G., Chanda, S., Van Remoortere, P., Symons, J.A., Fry, J., 2019. Antiviral activity, safety, and pharmacokinetics of AL-794, a novel oral influenza endonuclease inhibitor: results of an influenza human challenge study. J. Infect. Dis. 219, 177–185.

Yuan, P., Bartlam, M., Lou, Z., Chen, S., Zhou, J., He, X., Lv, Z., Ge, R., Li, X., Deng, T., Fodor, E., Rao, Z., Liu, Y., 2009. Crystal structure of an avian influenza polymerase PA(N) reveals an endonuclease active site. Nature 458, 909–913.